

PHASE TRANSITION PROCESS OF THE SUPERIONIC PHASE IN INORGANIC GLASS-COATED AgI NANOPARTICLES

H. YANG^a, X. P. LIU^b, Z. R. GE^b, R. H. CHEN^b, H. Z. TAO^{b*}

^aState Key Laboratory of Silicate Materials for Architectures, Wuhan University of Technology, Wuhan 430070, China.

^bJiangsu Ruihe Abrasives co., ltd., Yancheng 224051, Jiangsu, China

Solid-state ionic conductors are actively studied in recent years for their large application potential in electrochemical devices. As well-known, AgI is a super-ionic conductor for which the high-temperature α -phase shows a high ionic conductivity. However, due to the existence of phase transition from α -AgI to the poorly conducting β -/ γ -AgI at about 147°C, its applications are limited. Here, the ball-milling was employed to prepare the AgI nanoparticles coated with P₂S₅ glass. The phase transition temperature of α - to β -/ γ -AgI shifts considerably to lower temperature with the addition of P₂S₅. Stabilization of the α -AgI to low temperature should be ascribed to the nanosize scale AgI grains coated by inorganic glass, when prepared by ball-milling. The stabilized superionic phase reported here suggests the promising applications in Ag-base electrochemical devices.

(Received February 18, 2017; Accepted April 13, 2017)

Keywords: AgI, phase transition, ball mill

1. Introduction

Super-Ionic conductor materials are solid-state systems that have ionic conductivity, for operating electrochemical devices such as batteries and sensors. Comparing to the liquid phases, which can give high ionic conductivity as well, solid-state materials are much more suitable for the development of device fabrication, stability and safety. Silver-based ionic solid have been considered as an active component of electrochemical devices, because of its high conductivity and the high polarizability of Ag⁺ ions, which results in a high exchange rate at the electrode^[1-7]. AgI in α -phase is a typical super-ionic conducting material. Unfortunately, this phase is stable only above 147°C, and transforms at the temperature to β -/ γ - phase, which has very poor ionic conductivity. The origin of the ionic conductivity in α -AgI is that in which Ag⁺ ions are more or less statistically distributed over several possible sites in an I occupied bcc unit cell^[8-15].

Efforts to achieve high conductivity at lower temperature have focused on forming solid solutions or the synthesis of ternary phases. Shahi and Lee et al. in the papers reported the formation of α -AgI to be stable at room temperature in a AgI-Ag₂O-B₂O₃ glass by rapid melt-quenching techniques^[16,17]. However, in this case, low-temperature stabilization of α -phase is irreversible and the phase disappears at 110°C on second cooling after the first thermal cycle.

Another way to decrease the α - to β -/ γ -AgI transition temperature is to fabricate nanoscale AgI materials. With the size of the materials being down to nanoscale, the proportion of surface atoms increase results in an increase of surface energy as well. Therefore, the temperature of lattice fusion/melting and order-disorder phase transitions may be lowered^[18-20]. Guo et al. reported a solution-based method to produce polytype AgI nanoplates, for which α -AgI does not transform to β -/ γ -AgI at 147°C, but supercools by $\sim 50^\circ\text{C}$ ^[21]. Liang et al. developed a template-assisted technique for fabricating AgI/Ag heteronanowire that the high-temperature phase remained at temperature of 80°C^[9]. The investigation of Grabowski et al. shows, that there is a possibility to

*Corresponding author: clyde_yang@whut.edu.cn

stabilize the α -AgI to lower temperature by means of mechanosynthesis method^[22].

In this work, we have been able to synthesize AgI nanoparticles cladded by inorganic glass, in large quantities, by high energy ball-milling of $(1-x)\text{AgI}\cdot x\text{P}_2\text{S}_5$ system, which involves high energy milling and chemical reaction. The crystallization behavior and phase transition characteristics have been researched. In addition, we try to explore the origin of the decrease of the phase transition temperature for α -AgI to β -/ γ -AgI in this system and the effect of foreign phase in mixture.

2. Experimental

2.1 Sample preparation

The $(1-x)\text{AgI}\cdot x\text{P}_2\text{S}_5$ samples was synthesized by a high-energy planetary ball mill (Pulverisette-7 premium line; Fritsch, Idar-Oberstein, Germany) at 800 rpm for 20 hrs. The reagent-grade AgI (Aladdin) and P_2S_5 (Aladdin, Shanghai, China) crystalline powder, with different molar ratio $x(x=0.9, 0.5, 0.1)$ of $(1-x)\text{AgI}\cdot x\text{P}_2\text{S}_5$, was weighted and transferred into a 20 ml ZrO_2 pot according to the sample to ball(3 mm ZrO_2 balls in diameter) weight ratio of $\sim 1:15$. In addition, to avoid agglomeration during the milling process, 3 ml n-heptane was added into the pot as grind auxiliary agent. Then the pot was sealed with a silicone gasket and tightened to avoid air influx and contamination while the mixture was being milled. All the above processes were performed in a glovebox filled with dry N_2 gas. After milling, the powder was dried in a vacuum oven at 373 K.

2.2 Characterization

Phase compositions and structure of the as-prepared powder were characterized by X-ray diffraction method (RU-200B, Rigaku, Tokyo, Japan) with Cu K_α radiation at room temperature. To further explore their calorimetric response, designed up- and down-scanning programs with a DSC analyzer (DSC8000, PerkinElmer, Fremont, America) were carried out in the temperature range of 10-190°C with a typical sweeping rate of 10°C/min in N_2 .

3. Results

Similar to the reported AgI phase change process, β -/ γ -phase transforms into α -phase at 147°C (T_h , referring to the onset temperature of the endothermic effect) when heating at 10°C/min, while α - to β -/ γ -phase transition occurs at 142°C (T_c , referring to the onset temperature of the exothermic effect) when cooling at 10°C/min as shown in Fig. 1. When it comes to the as-milled pure AgI powder, T_h does not change; however, setting the milling time for 20hrs, T_c shifts from 142°C to 134°C at 600rpm and further to 130°C at higher rotation speed 800rpm.

To further modify the phase transition process of AgI, P_2S_5 was added. Series of $(1-x)\text{AgI}\cdot x\text{P}_2\text{S}_5$ mixed powder was synthesized by milling at 800rpm for 20hrs. When heating at 10°C/min (first upscan), compared to the pure AgI crystal and as-milled AgI powder a clear superheating effect (about 10°C) of the phase transition process for all the as-milled $(1-x)\text{AgI}\cdot x\text{P}_2\text{S}_5$ samples can be seen in Fig. 2.

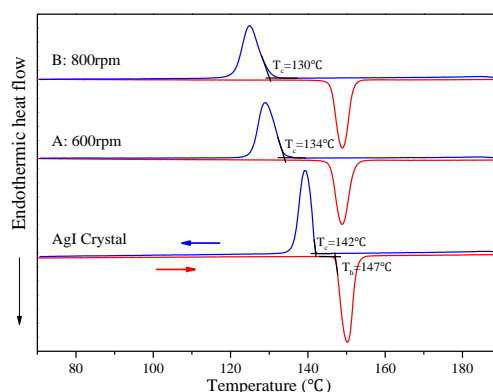


Fig. 1 Upscan and downscan DSC curves of the polycrystalline AgI and the as-milled AgI powder prepared at 600rpm (A) and 800rpm (B) for 20hrs. The upscan and downscan rates are 10K/min.

However, for the second and more upscans, the superheating effect disappears. That is to say, the phase transition temperature restore to the same temperature as that for the crystal AgI and as-milled AgI powder. When cooling at $10^{\circ}\text{C}/\text{min}$, compared to the as-milled pure AgI powder obtained at the same rotation speed (800rpm) and milling time (20hrs), T_c shifts to about 116°C , 60°C , and further to 47°C following the addition of P_2S_5 from 0.1, 0.5, to 0.9. The DSC curves of the third thermal cycle for the three samples ($x=0.1, 0.5$ and 0.9) are collected in Fig. 2(d). The difference of phase transition temperature between the heating (T_h) and cooling (T_c) branch, $\Delta T = T_h - T_c$, is marked in the graph. The right inset reveals that ΔT is a function of the amount of P_2S_5 addition: the more the P_2S_5 the larger the ΔT .

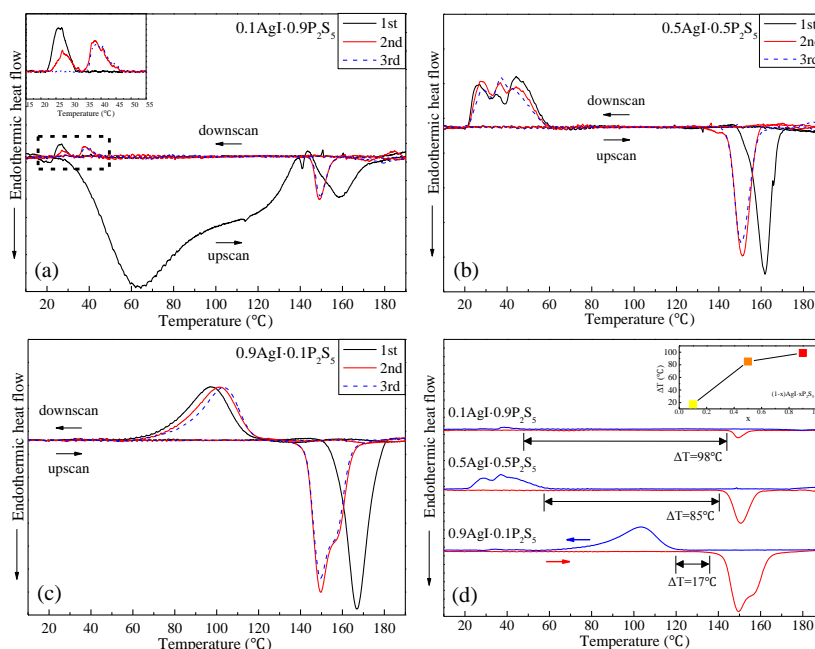


Fig. 2. Upscan and downscan DSC curves of sequential three thermal cycles for the as-milled $0.1\text{AgI}-0.9\text{P}_2\text{S}_5$ (a), $0.5\text{AgI}-0.5\text{P}_2\text{S}_5$ (b) and $0.9\text{AgI}-0.1\text{P}_2\text{S}_5$ (c) samples prepared at 800rpm for 20hrs. The upscan and downscan rates are 10K/min. Top inset in (a) shows the magnification of the curves in the marked area. (d) Upscan and downscan DSC curves of the third thermal cycle for the three samples. Right inset in (d) indicates composition dependence of hysteresis width ΔT (the difference of phase transition temperature between the heating (T_h) and cooling (T_c) branch).

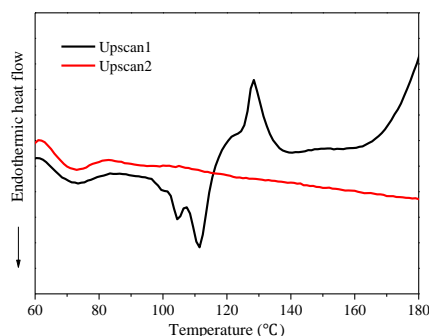


Fig. 3. DSC upscan1 curve of the P_2S_5 crystal powder at 10K/min up to 180 °C After naturally cooling to room temperature, DSC upscan2 curve was further recorded at 10K/min.

Furthermore, a broad endothermic reaction occurs in the range 30-140°C for the first heating process of as-prepared 0.1AgI-0.9 P_2S_5 sample, while it disappeared for the second and third upscans as shown in fig. 2(a). We attribute this phenomenon to the too much addition of P_2S_5 and milling method. It can be confirmed by the DSC curves of P_2S_5 crystal (Fig. 3).

To explore the structural original of the phase transition for the as-milled $(1-x)AgI \cdot xP_2S_5$ samples, X-ray diffraction method was carried out. As shown in Fig. 4, the halo pattern due to the amorphous state is observed in the 0.1AgI-0.9 P_2S_5 sample. Meanwhile, in the case of 0.5AgI-0.5 P_2S_5 and 0.9AgI-0.1 P_2S_5 samples, the lines ascribed to β/γ -AgI are detected. Rough estimation of a grain size in these two samples, based on Scherrer formula^[23], gives values 30-40nm.

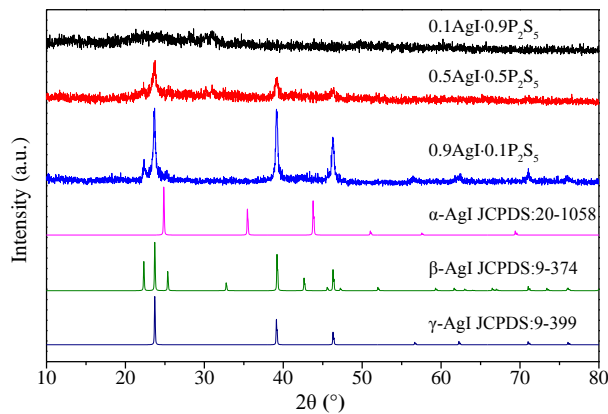


Fig. 4. XRD patterns of the as-milled $(1-x)AgI \cdot xP_2S_5$ samples prepared at 800rpm for 20hrs, together with α -AgI (JCPDS: 20-1058), β -AgI (JCPDS:9-374) and γ -AgI (JCPDS: 9-399).

4. Discussion

For the AgI samples prepared at 600rpm (A) and 800rpm (B) for 20hrs (Fig. 1), T_c shifts to lower temperatures with increasing milling speed. The faster the milling speed the smaller the AgI grains. Therefore, in fact, T_c is a function of a size of AgI grains, following the general relation: the smaller the grains the lower the T_c .

When P_2S_5 was added in the constitution, identical milling applied for the $(1-x)AgI \cdot xP_2S_5$ samples produce AgI nanoparticle coated by inorganic glass, which is the product of the reaction between AgI and P_2S_5 during high energy milling. The conclusion are supported by the XRD investigations in Fig. 4. No crystal line is observed for 0.1AgI-0.9 P_2S_5 sample, because the amount

of P_2S_5 is so much that AgI is almost coated or participates in chemical reaction to form amorphous phase. The lines ascribed to β/γ -AgI are detected in the $0.5AgI\cdot 0.5P_2S_5$ and $0.9AgI\cdot 0.1P_2S_5$ samples. The grain size in these two samples are 30-40nm.

As shown in Fig. 2, the endothermic reaction of β/γ -AgI to α -AgI transition for three samples are all superheated during the first heating process. It relates to some crystallization processes, with P_2S_5 existing, in high temperature. On heating above $147^\circ C$, the inorganic glass decomposes and the AgI grains begin agglomerate and grow, led to the thermal hysteresis. Especially, for $0.1AgI\cdot 0.9P_2S_5$ sample, this transition process was broad due to the effect of too much P_2S_5 . On the second and third heating, the T_h of the three samples are all restore to about $147^\circ C$ because most of the grown grains stop crystallization process after first heating run. In addition, from the second and third heating DSC curves of the $0.9AgI\cdot 0.1P_2S_5$ sample, two separate thermal events are observed, one at or near $147^\circ C$ and the other superheated by $10^\circ C$. This behavior can be described by the inhomogeneous size of AgI particles [10], having different transition behavior.

In the case of $0.1AgI\cdot 0.9P_2S_5$ sample (Fig. 2(a)), the broad, low temperature DSC endothermic peak during first heating are characteristic for the heterostructure of P_2S_5 . Compare with the DSC curves of P_2S_5 crystal (Fig. 3), the similar processes are observed. In Fig. 3, the presence of the endothermic peak at $65\text{-}85^\circ C$ is attributed to free sulfur melt. Meanwhile, the two overlapped endothermic peaks at $105^\circ C$ and $112^\circ C$ can be explained reasonably by the melt of little P_2S_5 and the transition for α -S to β -S. Exothermic peak at $130^\circ C$ can relate to crystallization enthalpy of amorphous P_2S_5 . Most of the reactions are irreversible process, so only the peak for melt of free sulfur exists in upscan2 curve. However, for $0.1AgI\cdot 0.9P_2S_5$ sample, milling method destroys the P_2S_5 crystal structure into another disorder state that results in a very broad $30\text{-}140^\circ C$ peak in the first heating DSC curve. Furthermore, the subsequent broad transition process is also affected by P_2S_5 .

In the cooling runs, the exothermic peaks of $0.1AgI\cdot 0.9P_2S_5$ and $0.5AgI\cdot 0.5P_2S_5$ (Fig. 2(a, b)), related to α - to β/γ -AgI transition, locate in a wide range of temperature and are overlapped and variational. These phenomena indicates that in result of the milling processing AgI and P_2S_5 react to form inorganic glass, which has heterogeneous structure characteristics to show up different thermodynamic performance for every thermal cycle. On the other hand, α -AgI phase is stable down to the low temperature. For $0.9AgI\cdot 0.1P_2S_5$ cooling (Fig.2 (c)), multiple heating/cooling cycling causes the temperature of the maximum of the peak to increase, in result, narrowing the range of stability of the α -AgI phase. This effect can relate to the inorganic glass decomposing and some crystallization processes causing the AgI grains to agglomerate and grow^[24], which occurs during heating process time after time.

The as-milled $(1-x)AgI\cdot xP_2S_5$ samples all show the thermal hysteresis in the α - to β/γ -AgI phase transition. The α -AgI grains are coated by the inorganic glass. Highly mobile Ag^+ existed at the interface between the nanoparticles and the coated phase could diffuse into latter, whereas I^- ions remain on the surface of the nanoparticle^[3]. Hence a larger number of lattice defects generates, which cause a charge imbalance. We attribute the suppression of the phase transition from the α - to β/γ -AgI on cooling not only to the increase of the surface energy, but also to the presence of such defects and the accompanying charge imbalance. As a result, phase transition hysteresis could relate to the coated level of AgI nanoparticle. As shown in Fig. 2(d), ΔT increases with the P_2S_5 addition increasing. Foreign phase involved in the milling process is beneficial to the low temperature stabilization of α -AgI.

In addition, the DSC peaks on cooling are all broad in Fig. 2. To rationalize this phenomenon, we note the theory has been reported of inhomogeneities within nanoparticles^[25]. For larger-size nanoparticles, they can be divided into two parts, the surface and an inner core. By the generation of defects, the surface region is strongly affected, whereas the core part is more like bulk AgI. Therefore, the phase transition starts at the inner part and then shifts gradually to the surface part, resulting in the broad peaks.

Enough small size of the AgI grains is crucial for the stabilization of the α -phase to low temperature. But nanoscale size AgI grains cannot be produced by direct milling method. Foreign

phase plays an important role in this process. For the mixture of AgI and P₂S₅, after milling, AgI nanoparticles are dispersed and coated by the inorganic glass, terminated agglomerating and growing. Furthermore, we suggest that AgI participates in the reaction forming amorphous product, which next decomposes producing AgI nanoparticles^[22].

5. Conclusions

The ball-milling method applied to the AgI-P₂S₅ systems with high AgI contents, forms the materials in which AgI nanoparticles allow to stabilize the α -AgI to temperature far below 147°C for multiple thermal cycles. The effective powdering of AgI by ball-milling up to nanosize scale is achievable only in foreign phases presence. The α -AgI stability range increase with the P₂S₅ addition increasing.

Acknowledgments

This work was financially supported by NSFC (No.51372180), the Key Technology Innovation Project of Hubei Province (2016AAA029) and Innovation and entrepreneurship leading talent for Yancheng city and Jiangsu province. We also thank Xiujian Zhao (Wuhan University of Technology) and Yuanzheng Yue (Aalborg University) for valuable discussions.

References

- [1] H. Chen, H. Tao, Q. Wu, and X. Zhao, *J. Am. Ceram. Soc* **96**, 801 (2013).
- [2] K. Terabe, T. Hasegawa, T. Nakayama, and M. Aono, *Nature* **433**, 47 (2005).
- [3] S. Hull, *Rep. Prog. Phys* **67**, 1233 (2004).
- [4] A. Qiao, H. Z. Tao, Y. Z. Yue, *J. Am. Ceram. Soc* **100**, 968 (2017).
- [5] X. Han, H. Tao, L. Gong, X. Wang, X. Zhao, and Y. Yue, *J. Non-cryst. Solids* **391**, 117 (2014).
- [6] H. Z. Tao, Z. Y. Yang, and P. Lucas, *Opt. Express* **17**, 18165 (2009).
- [7] S. Yan, H. Xiao, X. Liu, *Chalcogenide Lett* **13**, 483 (2016).
- [8] K. Funke, *Prog. Solid State Chem* **11**, 345 (1976).
- [9] C. Liang, K. Terabe, T. Hasegawa, M. Aono, and N. Iyi, *J. Appl. Phys* **102**, 124308 (2007).
- [10] Y.-G. Guo, J.-S. Lee, and J. Maier, *Solid State Ionics* **177**, 2467 (2006).
- [11] J.-S. Lee, S. Adams, and J. Maier, *J. Phys. Chem. Solids* **61**, 1607 (2000).
- [12] C. Lin, H. Tao, X. Zheng, R. Pan, H. Zang, and X. Zhao, *Opt Lett* **34**, 437 (2009).
- [13] H. Tao, C. Lin, S. Gu, C. Jing, and X. Zhao, *Appl. Phys. Lett* **91**, 475 (2007).
- [14] G. Dong, H. Tao, X. Xiao, C. Lin, Y. Gong, X. Zhao, S. Chu, S. Wang, and Q. Gong, *Opt. Express* **15**, 2398 (2007).
- [15] J. Zhang, J. Shen, C. Wei, H. Tao, and Y. Yue, *J. Solid State Electrochem* **20**, 1 (2016).
- [16] K. Shahi and J. Wagner, *J. Electrochem. Soc* **128**, 6 (1981).
- [17] J. S. Lee, S. Adams, and J. Maier, *J. Electrochem Soc* **147**, 2407 (2000).
- [18] H.Z. Tao, T.D. Bennett, Y.Z. Yue, *Adv. Mater* (DOI: 10.1002/adma.201601705).
- [19] S. Liu, Y. Kong, H. Tao, and Y. Sang, *J. Eur. Ceram. Soc* **37**, 715 (2016).
- [20] H. Tao, X. Zhao, and Q. Liu, *J. Non-Cryst. Solids* **377**, 146 (2013).
- [21] Y. G. Guo, J. S. Lee, and J. Maier, *Adv. Mater* **17**, 2815 (2005).
- [22] P. Grabowski, J. Nowiński, J. Garbarczyk, and M. Wasiucioneck, *Solid State Ionics* **251**, 55 (2013).
- [23] A. Patterson, *Phys. Rev* **56**, 978 (1939).
- [24] P. Grabowski, J. Nowinski, M. Holdynski, J. Garbarczyk, and M. Wasiucioneck, *J. Non-cryst. Solids* **408**, 66 (2015).
- [25] R. Makiura, T. Yonemura, T. Yamada, M. Yamauchi, R. Ikeda, H. Kitagawa, K. Kato, M. Takata, *Nat. Mater* **8**, 476 (2009).